EFFECTS OF COMPRESSION RATIO ON TURBULENCE KINETIC ENERGY AND DISSIPATION IN THE SUCTION STROKE OF A FOUR STROKE INTERNAL COMBUSTION ENGINE

M. M. Syed Ali and S. M. Nazrul Islam*
Dept. of Mechanical Engineering, BIT Khulna, Bangladesh.
*Dept. of Mechanical Engineering, BUET, Dhaka, Bangladesh.
S.M. Sapuan and H. M. Megat
Dept. of Mechanical and Manufacturing Engineering,
UPM, 43400 Serdang, Selangor, Malaysia

Abstract Turbulence kinetic energy and dissipation in suction stroke air inside a cylinder has been computed with five different compression ratios at 1000 rpm in a four stroke IC engine. The results of the computational works shows that turbulence kinetic energy in suction stroke starts increasing from the suction valve fully opening timing at 200^o crank angle after top dead centre (the reference TDC at 180^o) till the middle of the suction stroke at 255^o crank angle in all compression ratios and then found to decrease till bottom dead centre (BDC) when suction valve starts closing near bottom dead centre (at crank angle 340^o).The increase of compression ratio provides a predictable increases of the peak turbulence kinetic energy. Energy dissipation is also found to increase similarly from suction valve fully opening timing (at crank angle 200^o) to a peak value at the middle of suction stroke (at crank angle 240^o) when piston moves downwards and then found to decrease till the end of suction stroke when suction valve closes and follows a similar variation of turbulence kinetic energy generation. The increase of compression ratio also increase the energy dissipation of suction air inside the cylinder.

Keywords: Turbulence, dissipation, engine compression ,

INTRODUCTION

Air and fuel mixing in suction stroke of an IC engine depends on physical and chemical properties of fuel and flow property of the air and fuel also. Air fuel mixing depends on air velocity and turbulence. Several investigators computed the flow property of air in different models both in computational and experimental works. Normally turbulence and rotational motion called **swirl** is generated on the intake air-fuel mixture during suction stroke. Near the end of compression stroke, two additional mass motions are generated:

squish and **tumble**
Due to high speed of the engine, all flows into, out of engine cylinders are turbulent flows. The exception to those flows are in the corners and small crevices of combustion chamber where the close proximity of the wall dampens out turbulence. As a result of turbulence, thermodynamic transfer rates within an engine are increased by order of magnitude. Heat transfer, evaporation, mixing, and combustion rates all increase. As engine speed increases, flow rates increase, with a corresponding increase in swirl, squish, and turbulence. This increases the real-time rate of fuel evaporation, mixing of the fuel vapour and air, and combustion. When flow is turbulent, particles experience random fluctuations in motion can be super-imposed on their main bulk velocity. These fluctuations occur in all directions, perpendicular to the flow and in flow direction. This makes it possible to predict the exact flow conditions at any given time and position. Statistical averaging over many engine cycles gives accurate average flow conditions, but cannot predict the exact flow of any one cycle. The result is cyclic variations in operating parameters within an engine (e.g. cylinder pressure, temperature and burn angle).

For supersonic flows with shocks-induced three dimensionality, a great deal more research has been performed, although very few turbulence data have been reported. Yanta et al. (1982) and Ausherman et al. (1984) tested a 7^o semi-vertex angle sharp cone for angles of attack of 0^o , 2^o , and 4^o at a Mach number of 3. A laser Doppler velocity meter (LVD) was used to measure all tree velocity components and full Reynolds stress tensor. They found that the u'^2 turbulence intensities were little affected by the roll angle or angle of attack, that is with increasing three dimensionality. The v'^2 turbulence intensities were relatively constant across boundary layer on downward side and showed some increase with roll angle while w'^2 was insensitive to changes in each roll angle or angle of attack which has also been found in subsonic studies of three-dimensional boundary layers (Bradsaw & Pontokos 1985). The other two shear stresses were very small and only the $\rho u' v'$ stress exhibited increases near the wall when roll angle and angle of attack were increased.

Turbulence data were also obtained in a Mach number 2.85 in a cylinder flow by Kussoy et al. (1987) and Brown & Kussoy (1988). The three-dimensionality was generated by setting the cone at different angles of attack relative to the upstream cylinder. A strong shock was formed which separated the boundary layer. The LVD data include u', and v', measurement for two different angle of attack as expected, higher angles of attack lead to stronger shocks and turbulence kinetic energy was amplified accordingly.

Turbulence is the most difficult, unsolved theoretical problems in fluid mechanics. Nevertheless, there are different approaches in dealing with engineering problems. The simplest way is to take so-called turbulent viscosity or turbulent diffusivity as a constant property which was used in some earlier hydraulic and combustor flow predictions, Lixing.

A number of different models for turbulence can be found in fluid mechanics, Hinze (1975), which can be used to predict flow characteristics. One simple model uses fluctuation velocities u' in the X direction, v', in the Y direction and w' in the Z direction. These are superimposed on average bulk velocities of U, V, W in the X, Y, Z directions, respectively. The level of turbulence is then calculated by taking the root-mean-square average of u', v', and w'. The linear average of u', v', and w' will be zero.

There are many levels of turbulence within an engine. Large-scale turbulence occurs with eddies on the order of the size of the flow passage (e.g. valve opening, diameter of the intake runner, height of volume clearance, etc.). These fluctuations are random but have a directionality controlled by the passage of flow. On the other extreme, the small scale turbulence is totally random and homogeneous, with no directionality and controlled by viscous dissipation. There are all levels of turbulence in between these extremes, with characteristics ranging from those of small-scale turbulence to those of large-scale turbulence. The role of turbulence in internal combustion engine has been examined in a great deal and highly recommended for more in-depth study, Heyhood (1988).

To maximise air flow in the engine, the inside surface of most intake manifolds is made as smooth as possible. An exception to this concept is applied to the intake manifolds of the engines on some economy vehicles where high power is not desired. The inside surfaces of these manifolds are roughened to promote higher turbulence levels to enhance evaporation and air fuel-mixing. Though turbulence enhances evaporation and combustion but negative result of high turbulence is that it enhances the convection heat transfer to the walls in combustion chamber. The high heat loss lowers the thermal efficiency of the engine.

In finite volume technique, a mesh of quadrilateral elements can be used. The unknowns are not computed at the apices of those quadrilaterals but at their centres. To obtain a discretized form of a system, that system can be integrated on each element. MacCormack (1976) initially proposed an explicit scheme with splitting of the space operators to discretize the differential equations for solution of Euler equations. That scheme as well as the boundary conditions used on the air-foil surfaces are fully described by J. A Essers (1981) . This technique has been successfully applied to transonic flows around lifting airfoils. Results obtained for two different airfoils were compared to the same mesh by Baker (1975) and Rizzi (1979) respectively using non-conservative over-relaxation and a finite-volume time dependent technique for solution of the unsteady Eulers equations. The agreement is quite good especially with the results of Rizzi (1979). The difference in shock position observed by Baker (1975) is probably due to the fact that he uses a non conservation discretization.

Turbulence intensity in the suction stroke enhances atomization, vaporization and mixing of air fuel mixture for better combustion in IC engine.

Objectives of Research Investigation

The present research work has the following objectives.

(i) To compute the turbulence kinetic energy and dissipation at different crank angle or at different time steps in the suction stroke of an IC engine.

(ii) To compare the effects of compression ratio on the turbulence kinetic energy and dissipation in suction and exhaust stroke of a four stroke IC engine.

(iii) To model combustion chamber for better combustion efficiency.

MATHEMATICAL MODELING

In the opinion of many fluid dynamists, the only practical method for engineering predictions in this century is method of turbulence modeling based on solving the Reynolds time-averaged equation or the transport equation of correlation terms. Turbulence modeling of Reynolds average equation is still considered as practical engineering tool. All presently known turbulence models have limitation; ultimate turbulence models yet to be developed. One of the most frequently used two-equation models is the k-ε model first proposed by Harlow and Nakayama (1967). The description of this model are followed by Jones and Launder (1972) and Launder and Spadling (1974). High Reynolds (Re)-number form of k-ε model has proven to be a powerful tool for the prediction of a wide variety of turbulent flows. However there is the necessity of introducing the so-called "wall-functions" to bridge the viscous and buffer layers in proximity to the solid walls so that the direct influence of viscosity is neglected.

Several investigators have compared predictions of the k-ε model with experimental observations. For instance, Ayad and Mankbadi (1988) used k-ε to calculate fully developed, turbulent channel flow. El-Mehlawy & Mankbadi (1990) considered sudden-expansion flow, Mankbadi (1989), and Schoenung et al. (1989) developing flow in a duct. The fully developed duct flow shows good agreement between the calculated velocity profile and the experimental data of Hussain and Reynolds (1975). The dependence of the centerline mean velocity on Reynolds number was compared with the data collected by Dean (978). The comparison indicated that the model becomes less accurate at low Reynolds numbers.

For a sudden-expansion flow the k-ε prediction of the mean flow was compared with the data of Smyth (1979). The heat transfer is compared with data of Zemanick and Dougall (1970). The comparison shows good agreement between computation and prediction, with a predicted reattachment length, which is close to the experimentally determined one.

The exact transport equation of Reynolds stress can be obtained in the form of two terms on the left-hand side expressing the rate of change in convection due to mean motion respectively and five terms on right hand side expressing diffusion, stress, production, dissipation, pressure-strain correlation respectively. The summation of three normal stress components is related to the turbulence kinetic energy from where transport equation of turbulence kinetic energy can be derived. from u', v', and w' ..

In fact, not only the turbulence kinetic energy but also other turbulence properties are transported in the flow field. For example length scale has its own convection, diffusion, production and destruction. The stretch of large eddies (energy containing eddies) leads to the formation of small eddies and dissipation of small eddies (Kolmogorov eddies) leads to the formation of large eddies. Spadling and Launder (1972) summarized the second turbulence parameter as $Z= k^m/^n$, proposed by different authors. There have been different forms of two equation, such as k-f (Kolmogorov, $f= k^{1/2}l$), k-ε (Zhou, Harlow, Nukayama, $\varepsilon= k^{1/2}l$), k-l (Rodi, Spadling), k -κl (Ng., Spadling), k-w (Spadling, $w= k^{l/2}$) equation. A vast amount of predictions indicate that all the two-equation models give almost the same results. Among them the well known k-ε model is most widely used.

Physical Problem Description

As reference datum of crank angle, the bottom dead centre when exhaust valve opens has been assumed to be at 0.0 degree in exhaust stroke and top dead centre at the start of suction stroke has been assumed at 180 degree in suction stroke. The inside cylinder diameter has been taken 80 mm where piston moves in 1000 rpm.

The flow is entirely assumed to be turbulent and driven by the motion of the piston through intake and exhaust port over respective valve. The physical condition of the engine valve is transient (position is time dependent) which can be represented in CFD by dynamic-mesh feature namely 'event handling' moving grids and cell attachment/detachment) by setting up and solving simplified port-valve piston cylinder problem. The fluid inside the cylinder is assumed to be air and initially at room temperature and pressure commencing from BDC (bottom dead centre) and continues for 360^0 rotation of crank angle in each cycle starting from time step 0.0. The inert scalars with physical properties of air are used to track the intake and exhaust valve.

The Model Equations

Particularly k-ε model is used for high Reynolds number to fully turbulent incompressible or compressible flow, El Tahry (1983), Warsi (1981), Launder and Spadling (1974) and it allows to some extent for buoyancy effects Rodi (1979). The transport equations are as follows:

Turbulence energy

$$\frac{1}{\sqrt{g}}\cdot\frac{\partial}{\partial t}.\{\sqrt{g}\,\rho k\}+\frac{\partial}{\partial x_j}(\rho\,\tilde{u}_j\,k-\frac{\mu_{eff}}{\sigma_k}\cdot\frac{\partial u_k}{\partial x_j})=\mu_t$$

$$(P+P_B)-\rho\varepsilon-\frac{2}{3}(\mu_t\frac{\partial u_i}{\partial x_i}+\rho k)\frac{\partial u_i}{\partial x_i} \qquad (1)$$

Where,

$$P \cong 2\, s_{ij}\frac{\partial u_i}{\partial x_j}$$

$\mu_{eff} = \mu + \mu_t$

$P_B \cong g_i/\sigma_{h,t}\, 1/\rho\, \partial\rho/\partial x_i$

σ_k is empirical coefficient.

Turbulence dissipation rate

$$\frac{1}{\sqrt{g}}\cdot\frac{\partial}{\partial t}.(\sqrt{g}\,\rho\,\varepsilon)+\frac{\partial}{\partial x_j}(\rho\,\tilde{u}_j\,\varepsilon-\frac{\mu_{eff}}{\sigma_\varepsilon}\cdot\frac{\partial u_\varepsilon}{\partial x_j})=$$

$$C\varepsilon 1\cdot\frac{\varepsilon}{k}[\mu_t(P+C_{\varepsilon 3}P_B)$$

$$- 2/3 (\mu_t \frac{\partial u_i}{\partial x_i} + \rho \varepsilon k) \frac{\partial u_i}{\partial x_i}] - C_{\varepsilon 2} \rho \varepsilon^2 / k - C\varepsilon 4$$

$$(\rho\varepsilon \frac{\partial u_i}{\partial x_i}) \quad .... \quad (2)$$

Where

σ_ε, $C_{\varepsilon 1}$, $C_{\varepsilon 2}$, $C_{\varepsilon 3}$, $C_{\varepsilon 3}$ are further empirical coefficients whose value can be taken from experimental works, Launder and Spalding (1974), El Tahry (1983), Warsi (1981).

Modeling Strategy

Movement of the piston and valves of IC engine can be represented by moving mesh and changing cell connectivity to keep the dynamic parts of the grid so that cells can easily be changed during the transient phases. The mesh motion can be formulated in this problem by two conceptual steps. The first deals with connectivity changes i.e. cell removal, cell addition and reconnection which are defined as 'event'. The second step is to specify the grid vertex position as a function of time by supplying a set of grid manipulation commands to be executed at each time step.

The initial mesh contains all the cells which are used in the analysis of interest. Thus the overlapped cells at valve bottom position and valve top position should be initially represented in the grid construction. When cells are added (activated) they are still deemed to be reconnected to the neighbours and follow the process of deactivation by removal of cell from neighbours. Thus sequencing constraints of activation and deactivation are followed. If any part of the solution domain becomes separated from the rest of the flow field during transient phases, (e.g. intake port after intake valve closed) the cell material type there must be changed. So all material types are defined initially in the initial set-up.

RESULTS AND DISCUSION

The variations of turbulence kinetic energy of intake air for five different engine compression ratios have been computed and presented in graphical form in Figure 1 to Figure 5 and their comparison has been shown in Figure 6. Similarly the variations of energy dissipation are represented in Figure 7 to Figure 11, and their comparisons are depicted in Figure 12.

The results of the computational works (Figure-1 to Figure 5) show that turbulence kinetic energy in suction stroke starts increasing from the suction valve fully opening timing at 200^o crank angle after 20^o of the top dead centre (TDC at 180^o) till the middle of the suction stroke at 225^o crank angle for the both compression ratio and then found to decrease till bottom dead centre (BDC) at crank angle 340^o when suction valve is completely closed near bottom dead centre. The comparison of peak turbulence kinetic energy for five different compression ratios as depicted in Figure 6, shows that the increase of compression ratio from 7.5 :1 to 13.5: 1 provides a predictable increases of the peak turbulence kinetic energy from 2.06E+00 m^2/s^2 to 6.9 E+00 m^2/s^2 .

Dissipation energy is also found to increase (Figure 7 and Figure 11) similarly from suction valve fully opening timing at crank angle 200^o to a peak value peak value at the middle of suction stroke at crank angle 230^o when piston moves downwards but found to decrease till the end of suction stroke at crank angle 340^o when suction valve completely closes and follows a similar variation turbulence kinetic energy generation. The Figure 12 shows that increase of compression ratio also increase the peak value in dissipation of suction air inside the cylinder.

NOTATIONS

δ_{ij}	Kroneker delta =1 when i=j and zero otherwise.
k	Turbulent kinetic energy (TE)
κ	Empherical constant.
ε	Dissipation-rate.
μ	Fluid viscosity.
μ_t	Turbulent viscosity.
μ_e	Effective viscosity.
τ	Shear stress.
τ_{ij}	Stress tensor components.
ν_t	Eddy viscosity.
σ	Prandtl constant.
σ_ε	Empirical constant.
$C\varepsilon 1$,	Empirical constants
$C\varepsilon 2$ …	Empirical constants.
l	Length scale.
g	Standard gravitational. constant
ρ	Density.
ρo	Reference density.
t	Time.
u_i	Asolute velocity component in direction x_i.
u_j	Absolute velocity component in direction x_j.
$\tilde{u}_j$	$u_j - u_{cj}$, Relative velocity between fluid and local (moving) coordinate frame that moves with velocity u_{cj}.
$u_{i'}$	Fluctuating component of ui.
$u_{j'}$	Fluctuating component of uj.
s_{ij}	Rate of stress tensor.
s_m	Mass source.
s_i	Momentum source comp.

CONCLUSION

(i) The increase of compression ratio increases the turbulence kinetic energy and dissipation in suction stroke.

(ii) Turbulence kinetic energy and energy dissipation increase during the suction valve opening time at 200^o to middle of suction stroke (225^o -230^o) and then decrease till 340^o when suction valve starts closing.

(iii) After complete closing of the suction valve the turbulence kinetic energy and energy dissipation sharply decrease.

(iv) Higher compression ratio in a engine enhances the turbulence kinetic energy helping better air fuel mixing and better combustion efficiency.

REFERENCE

Ausherman, D. W. & Yanta, W. J., "Mach 3 three-dimensional boundary layer turbulence transport properties on a spherical blunt cone", AFWAL Viscous and Interacting Flow Field Effects. In Proc. 9th US Air Force and Federal Republic of Germany Data Exchange Agreement Meeting, pp. 155-178 (1984).

Ausherman, D. W. & Yanta, W. J., "Mach 3 Three-dimensional Boundary Layer Turbulence Transport Properties on a Spherical Blunt Cone", AFWAL Viscous and Interacting Flow Field Effects. In Proc. 9th US Air Force and Federal Republic of Germany Data Exchange Agreement Meeting, pp. 155-178 (1984).

Ayad, S.S., and Mankbadi, R.R., "A Study of Wake-Generated Unsteadiness in a Channel Flow Part I", The Mean Flow, in Forum on Unsteady flow Separation, K.N., Ghia, ed., ASME, pp. 231-239 (1988).

Baker, T. J., "The Computation of Transonic Potentials Flow", Computation Fluid Dynamics, VKI TN 109, (1975).

Brown J. D. Brown, J. L. & Kussoy, M. I., " A Docmentation of Two- and Three-dimensional Shock Separated Turbulent Boundary Layers". *NASA Tech. Mem*. 101008 (1988).

Dean, R.B., "Reynolds Number Dependence of Skin Friction and Other Bulk Flows Variables in Two-Dimensional and Rectangular Duct Flow", J. Fluids Eng., vol. 100, no. 2, pp. 215-223 (1978).

El-Mehllawy, F.M. and Mankbadi R.R., "Heat Transfer in Oscillating Flows", International Symposium on Nonsteady Fluid Dynamics, J. A., Miller and D.P. Telionis, eds., ASME, pp. 329-337 (1990).

Essers, J.A., "Application of a Fast Pseudo-unsteady Method to Steady Transonic Flows in Turbine Cascades", ASME Paper 81-GT-124, International Gas Turbine Conference, Houston, (March1981).

El Tahry, S.H., "k-ε Equation for Compressible Reciprocating Engine Flows", AIAA J. Energy, 7, No. 4 pp. 345-353 (1983).

Hussain A.K.M.F. and Reynolds W.C., "Measurements in Fully Developed Turbulent Channel Flow", J. Fluids Eng., vol. 97, no. 4, pp 568-580 (1975).

Harlow, F.M. and Nakayama, P.I., "Turbulence Transport Equations", Phys. Fluids, vol. 10, pp. 2323-2332 (1967).

Hinze, J.O., "Turbulence", New York, Mc. Growhill (1975).

Heyhood J.B. 1988 Internal Combustion Engine Fundamentals, New York, McGraw-Hill, 1988.

MacCormack, R.W., "An Efficient Numerical Method for Solving Time Dependent Compressible Navier Stroke Equations at High Reynolds Number", NASA TM. 73129; also in Computing in Applied Mechanics, Applied Mechanics Division, Vol. 18, ASME , New York, (1976).

Jones, W.P. and Launder, B.E., "The Prediction of Laminarization with a Two-Equation Model of Turbulence", Int. J. Heat and Mass Transfer, vol. 15, no. 2, pp. 301-314 (1972).

Kussoy , M. I. , Brown, J. D., Brown, J. L., Lockman, W. K. & Horstman, C. C., "Fluactuations and Massive Seperation in Three-dimensional Shock-wave Boundary Interactions", *Second Intl. Symp. on Transport Phenomena in Turbulent Flows*. pp. 875-887 (1987).

Launder B.E. and Spalding, D.B., "The Numerical Computation of Turbulent Flow", Compu. Meth. Appl. Mech. Eng., vol. 3, pp. 269-289 (1974).

Lixing, Z., Theory and Numerical Modeling of Turbulent Gas-particle Flows and Combustion, Dept. of Engineering Mechanics, Tsinghua University ISBN 0-8493-7721-8, CRC Press INC. Florida, USA. pp 123.

Mankabadi, R.R., “Study of Unsteady Rotor-Stator Interactions”, *J. Turbomachinery* , vol. 111, pp. 394-400 (1989).

Rizzi, A.W. and Viviand, H., “Results Submitted to the GAMM Workshop on Numerical Methods for Computation of Inviscid Transonic Flow with Shock Waves”, The Aeronautical Research Institute of Sweden, (Sept. 1979).

Rodi, W., “Influence of Bouncy and Rotation on Equation of Turbulent Length-scale”, Proc. 2nd Sym. on Turbulent Shear Flows (1979).

Schoenung, B., Mankbadi, R.R. and Rodi W., “Computational Study of the Unsteady Flow Due to Wakes Passing through a Channel,” *Turbulent Shear Flows*, Springer-Verlag, pp. 225-268 (1989).

Smith, R., “Turbulent Flow Over a Plane Symmetric Sudden Expansion”, *J. Fluids Eng*., vol. 101, no. 3, pp. 348-353 (1979).

Warsi, Z.V.A., "Conversation Form of Navier Strokes Equation in General Non-steady Coordinates”, AIAA J., 19, pp.240-242 (1981).

Yanta, W. J., Ausherman, D. W. & Hedlund, E., “Measurements of Three-dimensional Boundary Layer on Sharp Cone at Mach 3”, AIAA Paper 82-0289 (1982).

Zemanick, P. P. and Dougall, R.S., “Local Heat Transfer Downstream of Abrupt Circular Channel Expansion”, J. Heat Trans., vol. 92, no. 1, pp. 53-60 (1970).

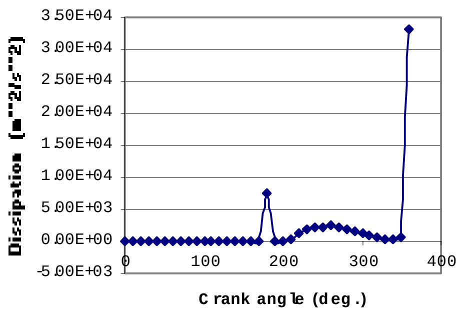

Fig.7 Crank angle Vs. Dissipation for compression ratio 7.5:1

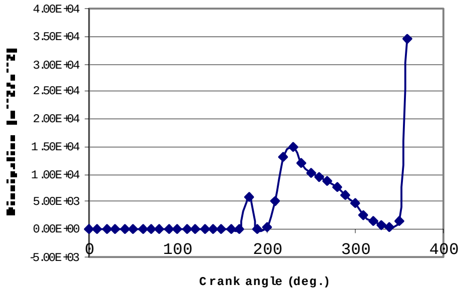

Fig.10 Crank angle Vs. Dissipation for compression ratio 12.0:1

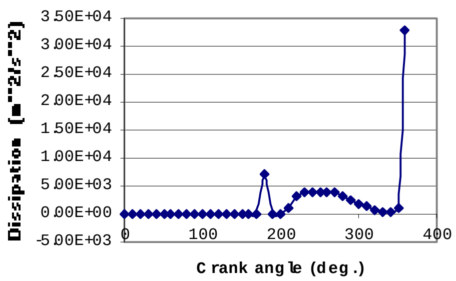

Fig.8 Crank angle Vs. Dissipation for compression ratio 9.0:1

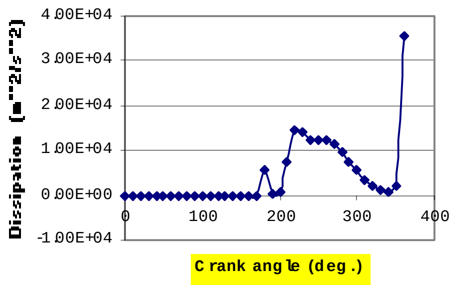

Fig.11 Crank angle Vs. Dissipation for compression ratio 13.5:1

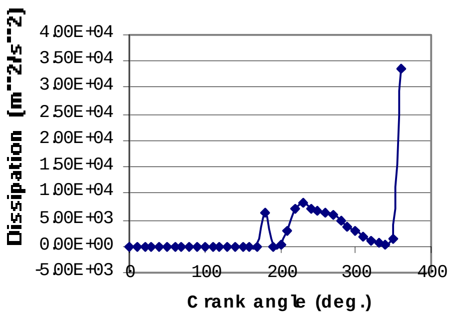

Fig.9 Crank angle Vs. Dissipation for compression ratio 10.5

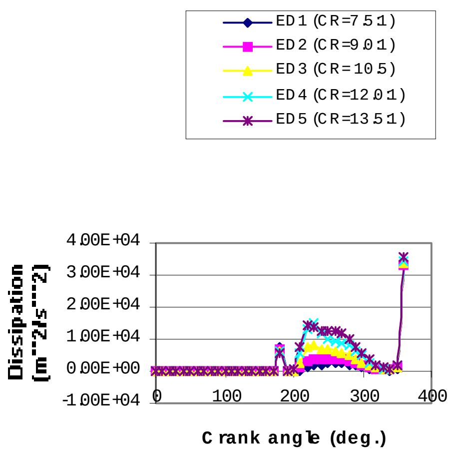

Fig.12 Comparision of energy dissipation at different compression ratios.

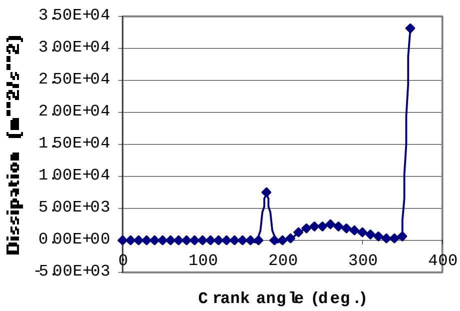

Fig.7 Crank angle Vs. Dissipation for compression ratio 7.5:1

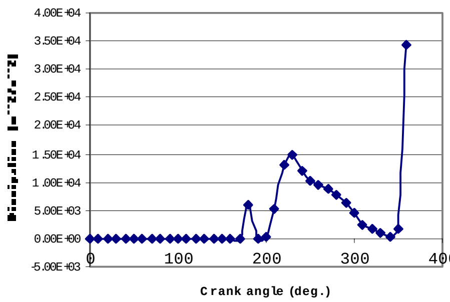

Fig.10 Crank angle Vs. Dissipation for compression ratio 12.0:1

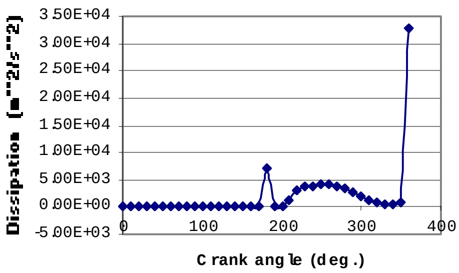

Fig.8 Crank angle Vs. Dissipation for compression ratio 9.0:1

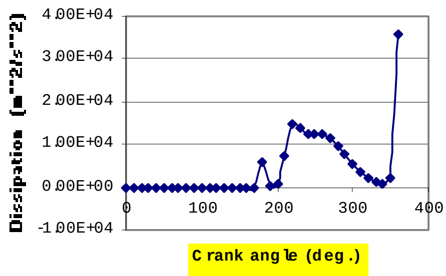

Fig.11 Crank angle Vs. Dissipation for compression ratio 13.5:1

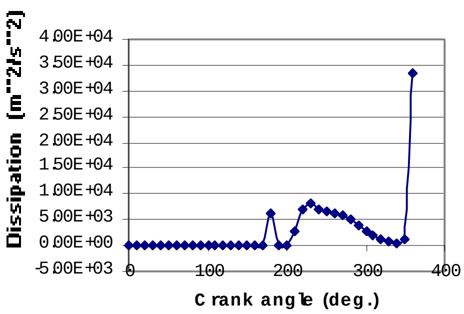

Fig.9 Crank angle Vs. Dissipation for compression ratio 10.5

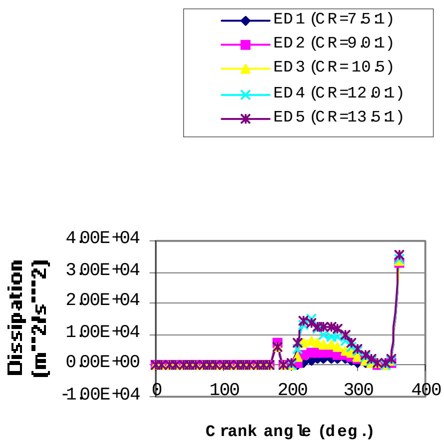

Fig.12 Comparision of energy dissipation at different compression ratios.